Author's Accepted Manuscript

Label-free Immunoassay for Porcine Circovirus type 2 based on Excessively Tilted Fiber Grating modified with Staphylococcal Protein A

Binbin Luo, Shengxi Wu, Wengen Zou, Zhonghao Zhang, Mingfu Zhao, Yong Liu, Shenghui Shi, Xiangfeng Xi, Zheng Zeng, Wangwang Liang, Zhijun Yan, Lin Zhang

Cite this article as: Binbin Luo, Shengxi Wu, Wengen Zou, Zhonghao Zhang, Mingfu Zhao, Yong Liu, Shenghui Shi, Xiangfeng Xi, Zheng Zeng, Wangwang Liang, Zhijun Yan and Lin Zhang, Label-free Immunoassay for Porcine Circovirus type 2 based on Excessively Tilted Fiber Grating modified with Staphylococcal Protein A, *Biosensors and Bioelectronic* http://dx.doi.org/10.1016/j.bios.2016.07.100

This is a PDF file of an unedited manuscript that has been accepted for publication. As a service to our customers we are providing this early version of the manuscript. The manuscript will undergo copyediting, typesetting, and review of the resulting galley proof before it is published in its final citable form. Please note that during the production process errors may be discovered which could affect the content, and all legal disclaimers that apply to the journal pertain.

Label-free Immunoassay for Porcine Circovirus type 2 based on Excessively Tilted Fiber Grating modified with Staphylococcal Protein A

Binbin Luo[a,c,d], Shengxi Wu[b*], Wengen Zou[a], Zhonghao Zhang[b], Mingfu Zhao[a], Yong Liu[c], Shenghui Shi[a], Xiangfeng Xi[e], Zheng Zeng[f], Wangwang Liang[f], Zhijun Yan[d], Lin Zhang[d]

[a]Chongqing Key Laboratory of Optical Fiber Sensor and Photoelectric Detection, Chongqing University of Technology, Chongqing, 400054, China
[b]School of Pharmacy and Bioengineering, Chongqing University of Technology, Chongqing, 400054, China
[c]School of Opto-electronic Information, University of Electronic Science and Technology of China, Chengdu, 610054, China
[d]Aston Institute of Photonic Technologies, Aston University, Birmingham, B4 7ET, UK
[e]National Research Center for Veterinary Medicine, Henan, 471003, China
[f]Chongqing Animal disease Prevention and Control center, Chongqing,401120, China

*Corresponding author. Tel.: +86-023-62563261 fax: +86-023-62563271. E-mail address: sxwu2004@cqut.edu.cn.

Abstract
Using excessively tilted fiber grating (Ex-TFG) inscribed in standard single mode fiber, we developed a novel label-free immunoassay for specific detection of porcine circovirus type 2 (PCV2), which is a minim animal virus. Staphylococcal protein A (SPA) was used to modify the silanized fiber surface thus forming a SPA layer, which would greatly enhance the proportion of anti-PCV2 monoclonal antibody (MAb) bioactivity, thus improving the effectiveness of specific adsorption and binding events between anti-PCV2 MAbs and PCV2 antigens. Immunoassay experiments were carried out by monitoring the resonance wavelength shift of the proposed sensor under different PCV2 titer levels. Anti-PCV2 MAbs were thoroughly dissociated from the SPA layer by treatment with urea, and recombined to the SPA layer on the sensor surface for repeated immunoassay of PCV2. The specificity of the immunosensor was inspected by detecting porcine reproductive and respiratory syndrome virus (PRRSV) first, and PCV2 subsequently. The results showed a limit of detection (LOD) for the PCV2 immunosensor of $\sim9.371 TCID_{50}$/mL, for a saturation value of $\sim4.801\times10^3 TCID_{50}$/mL, with good repeatability and excellent specificity.

Keywords: Label-free immunoassay; Excessively Tilted Fiber Grating(Ex-TFG); Porcine circovirus type 2 (PCV2); Staphylococcal protein A (SPA); Monoclonal antibody (MAb)

1. Introduction

In the past decades, thanks to advantages of compact, fast detection, high sensitivity and capacity of real-time measurement, various types of label-free optical fiber (OF) biosensors (Wang and Otto, 2013; Fan et al., 2008) have been developed for immunoassays, including taped OF fiber sensors for label-free detection of the immunoglobulin G (IgG) antibody (Tian et al., 2011), surface Plasmon resonance (SPR) biosensor for label-free immunoassay of anti-human IgG (Cao et al., 2013), and long-period grating (LPG) inscribed in photonic crystal fiber (PCF) for label-free monitoring of adsorbed/bound bio-molecules (He et al., 2011).

In a previous work, we reported a novel glucose sensor based on enzyme-immobilized excessively tilted fiber grating (Ex-TFG) inscribed in standard single mode fiber (SM28 fiber) (Luo et al., 2014), with the advantages of negligible thermal cross-talk effect, higher refractive index (RI) sensitivity, and higher Q-factor, compared with conventional LPG based biosensors, and no notable metal deposition needed in contrast to the SPR based ones. Herein, we used the Ex-TFG sensing platform to construct a novel type of immunosensor for the label-free, trace, and fast detection of porcine circovirus type 2 (PCV2).

PCV2, a minim single stranded DNA virus (12~23 nm) of mammals (Tischer et al., 1982), is the primary etiological agent of many diseases known as porcine circovirus-associated diseases (PCVAD), especially postweaning multisystemic wasting syndrome (PMWS) (Pejsak et al., 2010). Nowadays, PCV2 is universally considered the most important porcine infectious agent after swine fever and porcine reproductive and respiratory syndrome virus (PRRSV). Because of strong resistance, acid proof, and capability of spreading by copulation, ingestion or inhalation to repress the immunological function, PCV2 is commonly referred to as porcine AIDS (Ge et al., 2012).

Conventionally, laboratory detection methods for PCV2 include indirect immunofluorescence assay (IFA) (Gilpin et al., 2003), enzyme-linked immunosorbent assay (ELISA) (Ian et al., 2000), in situ hybridization (ISH) (Eva et al., 2007). Currently, many polymerase chain reaction (PCR) based methods (Caprioli et al., 2006; Kathleen et al., 2009; Chang et al., 2014) have also been widely applied in the PCV2 pathogen detection. However, these methods are purely based on biochemical techniques, and their applications are somewhat limited due to many factors. For example, the flaws of PCR-based methods include long detection time and high technical requirements. The disadvantages of IFA, ELISA and ISH are that they require labels, which constitute

challenges in biomedical research due to negative disturbance on immune bio-reactions, time-consuming pretreatment, and/or high operation costs. In recent years, optical methods for the detection of PCV2 attract increasing attention from scientists. For instance, a SPR imaging assay was developed to measure PCV2 antibody levels in serum samples by using a recombinant capsid protein as the antigen, with a correlation coefficient of 0.911 (Park et al., 2011). Instead of assessing the PCV2 antibody, a label-free optoelectronic SPR immunoassay built with a biomembrane for detecting the PCV2 Cap protein was adopted for inspecting viruses in PCV2 sample solutions, and exhibited a limit of detection (LOD) of 0.04μg/mL (Hu et al., 2014).

In this work, we present a competitive label-free Ex-TFG biosensor immobilized with anti-PCV2 monoclonal antibody (MAb) through staphylococcal protein A (SPA), for specific and fast detection of PCV2 isolated from porcine lymph nodes and lung tissues. The proposed immunosensor was built through several surface-modified steps in a sequence that included silanization of the fiber surface, adsorption of SPA and immobilization of highly purified anti-PCV2 MAbs. The key factor for the surface modification was the formation of a molecular layer of SPA, a type I membrane protein extracted from *Staphylococcus aureus*, whose polypeptide chain is composed of A, B, C and D homologous regions that are capable of binding the IgG Fc fragment in serum of many mammal without affecting the bioactivity of the IgG Fab fragment (i.e. antigen-binding site) (Sjoquist et al., 1972). In addition, SPA could make the Fab antigen binding fragment of the antibody appear outside the SPA-molecular film and extend towards the outer flowing phase (Kangwa et al., 2015), thus greatly enhancing the proportion of anti-PCV2 MAb bioactivity and improving the effectiveness of specific binding in the immunoassay process. Immunoassay experiments were carried out *in vitro* by monitoring core-to-cladding mode coupling wavelength shift of the proposed Ex-TFG immunosensor. Using urea to break the bond between the anti-PCV2-MAb's Fc fragment and SPA molecule, the repeatability and possible reusability of the proposed immunosensor were investigated. Through control experiments first detecting PRRSV (non-specific) and PCV2 (specific) subsequently, excellent specificity was obtained for the immunosensor.

2. Material and fabrication

2.1. Fabrication of Ex-TFG and Experimental setup

Ex-TFGs were inscribed in H_2-loaded SM28 fiber by using the scanning mask technique and doubled frequency Ar^+ laser at 244 nm, with a power level of 150 mW. A custom-designed amplitude mask with a period of 6.6μm was employed for imprint. In order to introduce the excessively tilted structure, the amplitude mask was tilted at 78°, thus producing titled fringes at ~ 81° in the fiber core with a grating period of ~32μm along the fiber axis (Zhou et al., 2006). The grating length was around 12 mm. Fig. 1(a) shows the micrographic image of the excessively tilted fringes in the fiber core. The excessively tilted finings in the fiber core of Ex-TFG can induce a significant birefringence and couple the core mode to co-propagating cladding modes, thus resulting in dual-peak resonances that correspond to the two orthogonal polarization modes (i.e. 'fast-axis polarized mode' and 'slow-axis polarized mode') (Luo et al., 2014), whose spectra measured in air are shown in Fig. S1(a). Since the fabrication process is highly standardized, Ex-TFGs are relatively low cost, easily made and reproducible.

The experimental setup used for investigating the transmission spectrum of Ex-TFG sensor is shown in Fig. 1(b) and Fig. S1(b). Light from an output of a sweep laser light source (SLLS, 1510~1590 nm, 1Hz) integrated in a fiber optic grating demodulation system (FOGDS, MOI-SM125, wavelength accuracy of 1 pm) was launched into an SM28 fiber, and the transmission spectrum was recorded by another FOGDS channel. A fiber optic isolator (FOI) was used to isolate the backscattering and reflected light. A polarizer and a polarization controller (PC) were used to excite and maintain the light launching into Ex-TFG to operate in the fast-axis polarized mode, since its RI sensitivity is larger than that of the slow-axis polarized mode (Luo et al., 2014).

Fig. 1(c) shows the transmission spectrum at the 1535~1555 nm region when the fast-axis polarized mode is fully excited (i.e. slow-axis polarized mode fully suppressed), showing that the FWHM of the resonance spectrum is ~3.0 nm, which is far smaller than that of conventional LPG or SPR based scheme (usually >~20 nm and >~50 nm, respectively). Therefore, measurement accuracy of the Ex-TFG sensor is much higher than those of LPG or SPR counterparts. Furthermore, experimental results showed that RI and temperature sensitivity of the Ex-TFG was ~135.0 nm/RIU (RI 1.33~1.38) and ~4.6 pm/°C, respectively. Obviously, Ex-TFG has a much higher RI sensitivity, but a markedly lower temperature cross-talk effect compared with conventional LPGs (Shu et al., 2002). As a result, all the above features render Ex-TFGs a favorable platform for biochemical sensing.

2.2. Reagents

Analytical grade reagents and sterile deionized water were used for preparing all the working solutions. 3-aminopropyltriethoxysilane (APTES), N-Hydroxysuccinimide (NHS), bovine serum albumin (BSA), 1-ethyl-3-[3-dimethylaminopropyl]carbodiimide hydrochloride (EDC), fluorescein isothiocyanate (FITC), polyethylene glycol (PEG-1500), hypoxanthine-aminopterin-thymidine (HAT) and hypoxanthine-thymidine (HT) supplemented medium were purchased from Sigma-Aldrich Company, China. 4-morpholineethanesulfonic acid hydrate (MES) (0.1M,
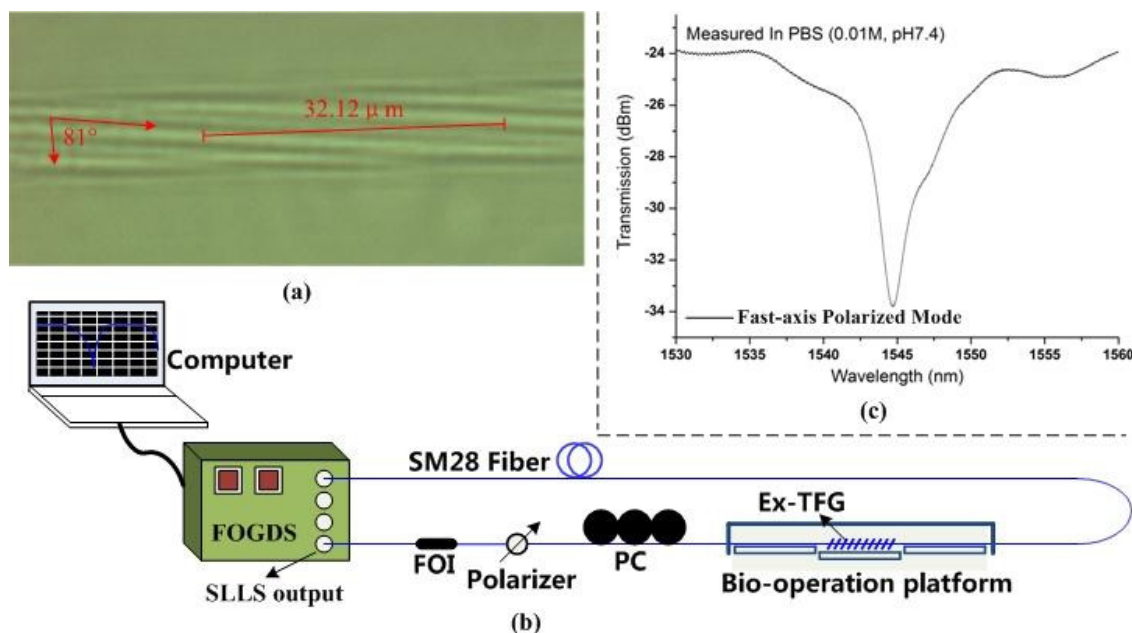
Fig. 1. (a) Micrograph of the Ex-TFG's core region, (b) Experimental setup, (c) Spectrum centered in 1535~1555 nm as the fast-axis polarized mode fully excited.

pH5.5~6.7) buffered solution and urea were purchased from Shanghai General Chemical Reagent Factory (Shanghai, China). Tris, glycine, isopropyl-β-D-thiogalactoside (IPTG) and lysozyme were purchased from Gen-View Scientific Company, USA. Phosphate buffered solution (PBS) (0.01M, pH7.4) and mouse IgG were purchased from Wuhan Boster Biological Technology Company, China. *Staphylococcus aureus* (strain 1.800), purchased from the Chinese Academy of Sciences, was used for SPA extraction and purification. The pTO-T7 vector was kindly provided by the National Research Center of Veterinary Medicine, China. The sample solution of PCV2 ($10^{6.5}$ $TCID_{50}$/mL, i.e. 1.37 mg/mL) isolated from lymph nodes and lung tissues of PCV2-infected pigs, as well as PRRSV were kindly provided by Chongqing Engineering Research Center of Prevention and Control of Swine Infectious Diseases, China. $TCID_{50}$/mL was used in this study as the dosage unit to represent the concentration of PCV2, and this is of more significance than using ng/mL, because $TCID_{50}$/mL refers to the 50% tissue culture infective dose, which represents the actual infectivity of virus. The obtained PCV2-contained sample solution was diluted by PBS (0.01M, pH7.4) to different titer levels (1.173, 2.331, 9.371, 2.308×10^2, 5.771×10^2, 1.154×10^3, 1.846×10^3, 2.308×10^3, 4.801×10^3 and 1.154×10^4 $TCID_{50}$/mL) for immunoassays; the relationship between PCV2 titers and the corresponding concentrations is shown in Table S2.

2.3. SPA Extraction and purification

Staphylococcus aureus, strain 1.800, was first cultured in nutrient broth for 24 h. Then, 0.05M Tris-HCl (pH 7.5) was used to wash the bacteria. Lysozyme was added at 5 mg per 100g wet bacteria, with pH adjusted to 3.5. After centrifugation, the pH of the supernatant was adjusted to 7.0, and supernatant proteins were precipitated with saturated ammonium sulfate, re-dissolved in PBS, and transferred into a dialysis bag for dialysis. The dialyzed solution was purified on a mouse IgG-Sepharose 4FF affinity column (Fig. S2(a)). The adsorbed SPA was eluted with 0.1M HCl-Gly buffer (pH 2.7). The eluted samples were collected, combined, and dialyzed to concentrate for further analysis. SPA concentration was 0.933 mg/mL as detected by the BCA method. SDS-PAGE showed an obvious band at 42kD (Fig. S2(b)), in line with previous findings (Sjoquist et al., 1972; Kangwa et al., 2015). An indirect ELISA was developed to detect the reactivity of SPA with mouse IgG. The results showed that mouse IgG could still bind to SPA when diluted at 1:25600 (see Table S1), indicating that the extracted SPA possessed high activity.

2.4. Preparation and identification of the anti-PCV2 MAbs

The PCV2-ORF2 gene was amplified by PCR and cloned into the pTO-T7 vector to construct a recombinant expression plasmid, which was transformed into *E. coli*. The recombinant protein was induced by 0.2 mM IPTG at 28℃ for 10 hours and analyzed by SDS-PAGE. The results showed that the ORF2 coded Cap protein was highly expressed in *E. coli*, as shown in Fig. 2(a). The expressed Cap protein of PCV2 was denatured and purified by ion-exchange chromatography, and analyzed by SDS-PAGE and Western blot. A BALB/c mouse was immunized four times with the purified Cap protein, and spleen cells and SP2/0 cells were fused with PEG-1500; a cell fusion rate of 86.7% was obtained. An ELISA was developed to detect MAbs secreted by hybridoma cells, and a positive rate of 18.4% was obtained. One hybridoma cell line secreting MAbs, named 3G9, was developed by two subclones. After purification by ion-exchange and affinity chromatography, 15 mg of PCV2 Cap MAbs, with 94.60% purity at a concentration of 1.152mg/mL, was obtained (Fig. 2(b)). MAb specificity was identified by Western-blot (Fig.

2(c)). After repeated frozen storage, thawing, and generation, it could still steadily yielded high titers of the antibodies. In this assay, one high titer, specific MAb against the PCV2 Cap protein was successfully prepared, and may be useful in the development of a quick and specific method for PCV2 detection.
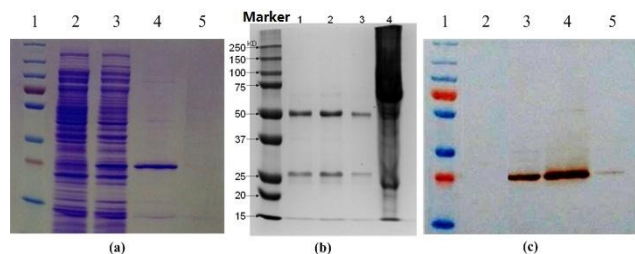

Fig. 2. Preparation and Purification of PCV2 MAbs. (a) Identification of PCV2 Cap by SDS-PAGE. Lane1, Protein molecular weight marker; lane 2, PCV Cap proteins expressed in *E. coli* without induction; lane 3, PCV Cap protein expressed in *E. coli* induced by IPTG; lane 4, PCV Cap protein purified by ion-exchange chromatography; lane 5, PCV2. (b) SDS-PAGE analysis of purified PCV2 MAbs from ascetic fluid. Lane 1-3, purified PCV2 MAbs. Heavy and light chains are shown; lane 4, unpurified ascetic fluid. (c) Identification of PCV2 MAbs by Western-blotting. From left to right, lane 1 to lane 5, same as in Fig. 2(a).

2.5. Surface modification for Ex-TFG

Ex-TFG was initially immersed in HNO_3 (5% v/v) for ~2h at ~40°C to remove contamination, and thoroughly washed by de-ionized water and ethanol. The cleaned Ex-TFG was then immersed in a H_2SO_4 solution (95% v/v in H_2O_2) for ~1h at room temperature to activate hydroxyl-groups on the fiber surface, followed by releasing the residual liquid droplets using a pipette and drying in a convection oven for ~6h at ~60°C. The silanization process was realized by immersing the –OH activated Ex-TFG in the APTES solution (10%v/v in absolute ethanol) for ~30 min at room temperature, where the APTES molecules would assemble to –OH groups, thus –NH$_2$ groups were available on the fiber surface. Then, the Ex-TFG sensor was washed with absolute ethanol and de-ionized water to thoroughly remove non-binding silane compounds, and dried in convection oven for ~20 min at ~37°C.

With the concept that EDC and NHS are widely applicable cross-linking reagent of carboxylates with amines (Andreeva et al., 1993; Hong et al., 2007). Herein, EDC (0.933 mg) was added into the highly purified SPA solution (0.311 mg/mL in MES, 1 mL, pH 6.0) first, and NHS (1.244 mg) subsequently, then the mixed liquor was keep in darkroom for ~25min at ~37℃. Afterwards, the silanized Ex-TFG was immersed in the activated SPA solution (0.3 mL, pH was adjusted to 7.2) for ~30 min at room temperature so as to form the linkage between carboxyl group of SPA and amino group of APTES, thus producing a SPA molecule layer, which was washed several times with PBS and air dried. Finally, the SPA-modified Ex-TFG was incubated in the highly purified anti-PCV2-MAb solution (0.08 mg/mL in PBS, phase volume 0.2 mL) for ~40 min at room temperature for anti-PCV2 MAb immobilization, and subsequently washed 3~4 times with PBS. The whole mechanism of chemical binding of anti-PCV2 MAb to the fiber surface is depicted in Fig. 3.

3. Results and Discussion

3.1. Surface modification monitored by resonance spectra of Ex-TFG

Utilizing the experimental setup in Fig. 1(b), the spectrum of Ex-TFG immersed in blank PBS (0.01M, pH7.4) was recorded after every step of surface modification. As shown in Fig. 4(a) and (b) (blue solid line), due to the adsorption of the
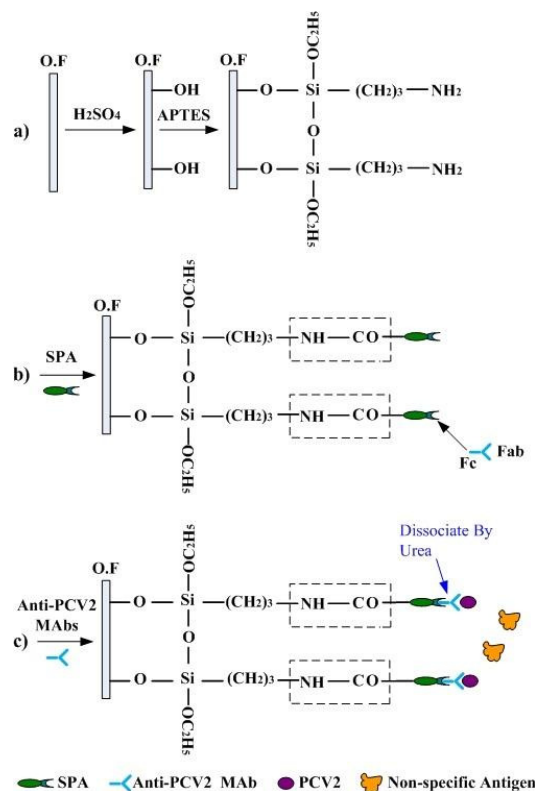
Fig. 3. Mechanism of linkage of (a) APTES, (b) SPA, (c) anti-PCV2 MAb on the fiber surface.

ATPES, SPA and anti-PCV2-MAb molecular layers, the sensor's resonance wavelength shifted ~0.345 nm, ~0.62 nm and ~0.765 nm compared with that (~1544.68 nm) of the bare Ex-TFG, respectively. This was expected because an additional layer on the fiber surface would affect the effective RI of cladding modes, leading to the core-to-cladding coupling resonance conditions to change (Zhou et al., 2006).

3.2. Surface characteristics of the silanized, SPA-modified and anti-PCV2 MAb immoblized Ex-TFG

A scanning electron microscope (SEM) (JSM-6460LV) was used to assess the coating consistency of APTES and SPA on the fiber surface. Fig. 5 (a), (b) and (c) are SEM micrograph (500×) with inset of the detail (5000×) for the bare, silanized and SPA-modified fibers, and the magnified images of the insets are shown in Fig. S3(a), S3(b) and S3(c), respectively. It is clear that the surface of bare fiber was smooth, but appeared to be plicated after silanization and SPA modification process, indicating that the methodology used for silanization and the subsequent SPA modification produced nicely adherent layers on the fiber surface. However, comparing Fig. 5(b) and (c) (or Fig. S3(b) and S3(c)), there were no obvious differences between them; thus, in order to give a more visual evidence of the SPA layer absorbed on the fiber surface, several bare fibers were also submitted to the modification process together with the Ex-TFG; for one of these, we used a prepared FITC-labeled-SPA solution for its SPA-modification step, in which the treating process and conditions were identical to those descried in section 2.5.

Inverted fluorescence microscopy (Olympus Venox) was used to assess FITC-labeled-SPA treated fibers, and strongly glowing fluorescence was observed, as shown in Fig. 5(d) and
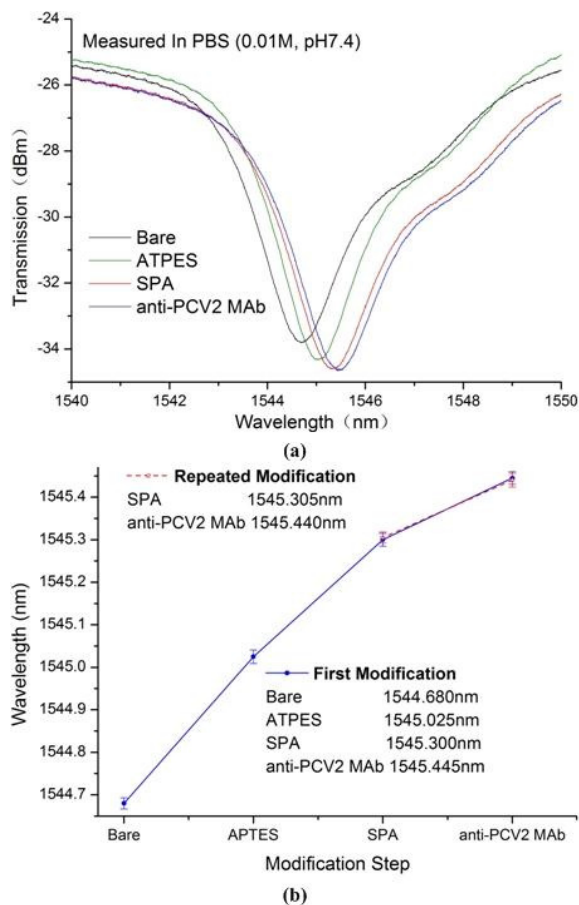
Fig. 4. (a) Spectrum evolution for the first surface modification. (b) The resonance wavelength shifts of the first surface modification (blue solid line) and repeated one (red dashed line).

Fig. S4(a), providing fairly good evidence to the consistent SPA layer established on the fiber surface. In a parallel experiment, silanized fibers (without SPA treatment) were also investigated under the same conditions, but no fluorescence was found (Fig. S4(b)). Hence, the fluorescence can be attributed to the presence of SPA molecules adsorbed on the fiber surface.

Given the widespread use of SPA for antibody immobilization in other types of immunosensors such as electrochemical (König et al., 1994) or piezoelectric (Wang et al., 2004) ones, the proposed SPA-modified technique for Ex-TFG should not be only confined in the detection of PCV2 but also could be extended to detecting other viruses or biomarkers related to serious human diseases.

3.3. PCV2 detection by the anti-PCV2-MAb immobilized Ex-TFG

The experimental setup is shown in Fig. 1(b). The anti-PCV2-MAb immobilized Ex-TFG was fixed on a home-made bio-operation platform consisting of two separated glass slides with a movable slide between them (Fig. S5). Initially, a blank PBS solution was introduced in the movable slide to cover the whole region of the sensor, and the observed resonance wavelength was recorded as the reference. Subsequently, the prepared PCV2-containing sample solutions (phase volume of200μl) of different titer levels were dropped carefully to cover the whole region of the sensor in turn. Spectrum evolution of the sensor was monitored throughout the immunoassay. At each titer level, it would take 5~10 min for
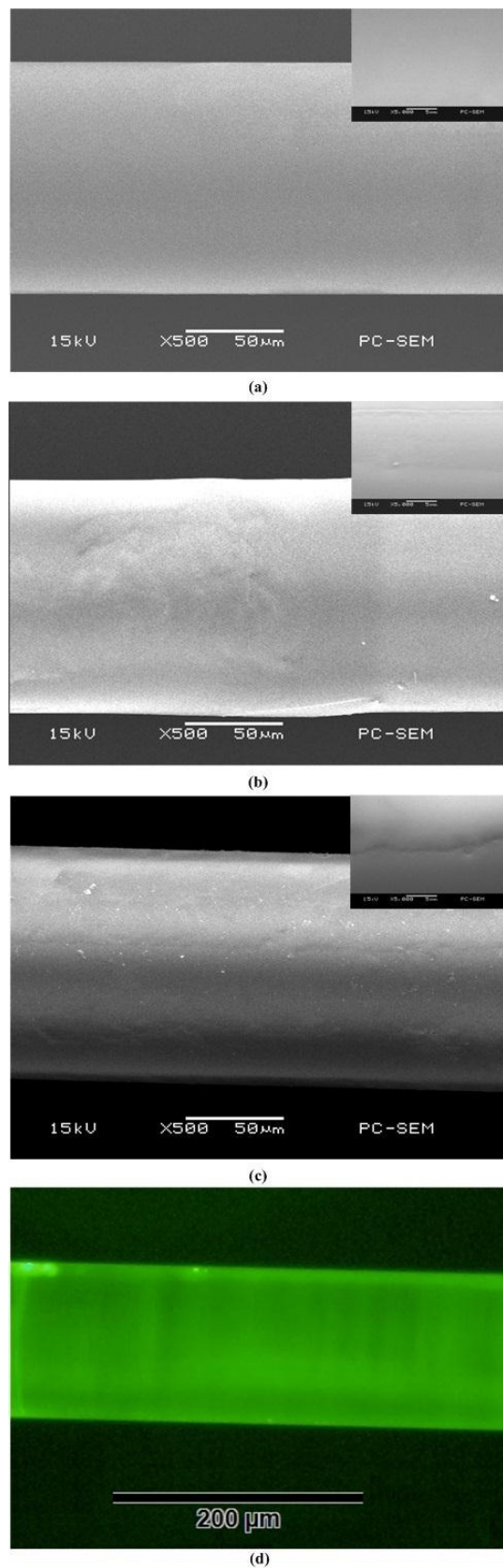
Fig. 5. Micrograph of the whole surface configuration of (a) bare fiber, (b) silanized fiber, and (c) SPA modified fiber under SEM (500×); Insets: detailed surface configuration (5000×). (d) Fluorescent image of the FITC-labeled-SPA modified fiber under an inverted fluorescence microscope.

the sensor spectrum to achieve a stable status, which signified a complete immunoreaction between the PCV2 antigens and anti-PCV2 MAbs. This was followed by washing of the sensor several times using PBS, for the preparation of the next titer-level test. Afterwards, the resonance wavelength of the senor immersed in a blank PBS solution was recorded as the desired data point of

the corresponding titer level.

The experimental results showed that the resonance wavelength was nearly unchanged as the minimum PCV2 dose in the sample solution was 1.173 TCID$_{50}$/mL or 2.331 TCID$_{50}$/mL, respectively, but an identifiable wavelength shift of about 0.02 nm could be observed at ~9.371 TCID$_{50}$/mL, as shown in Fig. 6(a) and (b) (Group 1). However, the red-shift of wavelength was saturated (~0.215 nm) for titer $\geq$~4.801$\times$10^{3} TCID$_{50}$/mL, which could be explained by the fact that the available Fab antigen binding fragment of anti-PCV2 MAbs was gradually occupied by PCV2 antigens as the test number increased. Therefore, the LOD of the proposed sensor was estimated to be ~9.371 TCID$_{50}$/mL (i.e. ~4.06 ng/mL), which is far lower than that (0.04μg/mL) obtained in a recently reported study employing optoelectronic SPR method (Hu et al., 2014). Besides, our immunosensor targeted the whole PCV2, the measurement unit of which is TCID$_{50}$/mL that represents the actual infectivity of virus, while the latter research detected the PCV2 Cap protein; therefore, our sensor is more significant than the latter.

3.4. Repeatability of the SPA-modified Ex-TFG

To assess the sensor's repeatability, the fully PCV2-combined Ex-TFG was soaked in urea solution (4M in de-ionized water, phase volume 1 mL, pH 6.5-7.0) for ~12h to thoroughly dissociate the linkage between the anti-PCV2 MAbs and SPA layer, as shown in Fig. 3(c). Subsequently, the above experiments, including re-immobilization of anti-PCV2 MAbs and PCV2 detection, were carried out once more with totally identical conditions. Effectiveness of anti-PCV2 MAb dissociation from the SPA layer and their re-immobilization on the sensor was evaluated by observed resonance wavelengths, as compared in Fig. 4(b) (red dashed line), which (~1545.305 nm and ~1545.440 nm) are nearly the same as those (~1545.3 nm ~1545.445 nm) of the first SPA-modified and anti-PCV2-MAb immobilized steps, respectively, revealing that anti-PCV2-MAb molecules were basically dissociated from the fiber surface but left the SPA layer still firmly attached. This was expected because urea is capable of effectively degenerating proteins, especially non-covalent binding proteins (Trang et al., 2016), not affecting the bioactivity and biological stability of SPA (Abani et al., 2002). Therefore, in this study we used urea to effectively dissociate anti-PCV2 MAbs from the SPA layer.

Finally, using an identical methodology for dissociation and re-immobilization of anti-PCV2 MAbs on the fiber surface, we carried out another three groups (Groups 3~5) of repeated experiments. Wavelength variations of the repeated experiments are shown in Fig. 6(b) (Groups 2~5) for comparison, suggesting that the wavelength variations slightly decline as compared with that of the first group, especially at high titer range (i.e. $\geq$5.771$\times$10^{2}TCID$_{50}$/mL). This is probably due to that the available quantity of binding anti-PCV2 MAbs is slightly less than that of the first anti-PCV2-MAb immobilization as a consequence of tiny losses of SPA in the
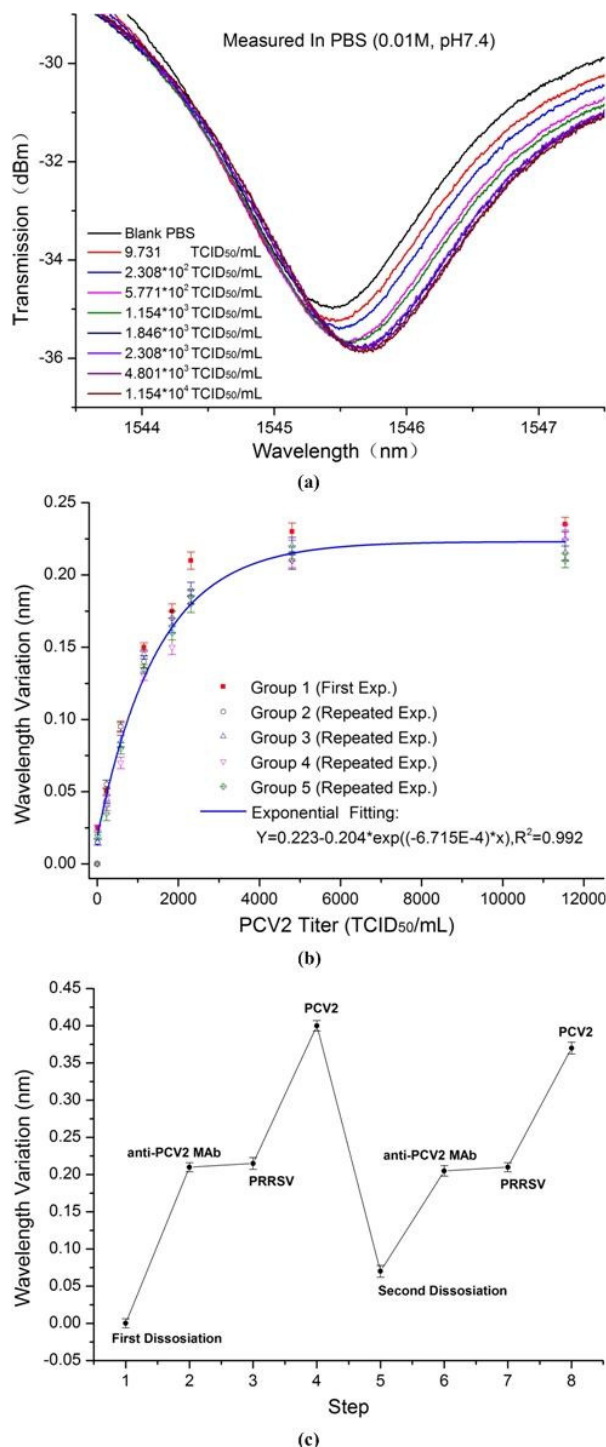
Fig. 6. (a) Spectrum evolution for the first group of PCV2 detection. (b) Resonance wavelength variation of the first group (Group 1) and repeated group of PCV2 detection (Group 2~5), and the fitting curve (blue line) of the relation between the wavelength variation and PCV2 titer. Relative standard deviation (RSD) for 5 different measurements: $0.038 < RSD < 0.15$. (c) Variations of resonance wavelength for the first and second specificity experiments of the sensor.

subsequent dissociation process. Nevertheless, the used dissociation method provides a good demonstration for the repeatability of the proposed sensor, once again confirming that the SPA layer was still firmly attached on the fiber surface and can effectively recombine with anti-PCV2 MAbs after treatment with urea solution.

Based on data of the first and repeated immunoassay experiments, the standard curve reflecting the relationship between the resonance wavelength variation of the Ex-TFG immunosensor and PCV2 titer could be deduced by using the exponential fit, as shown in Fig .6 (b)(blue line) as well, with a high R-square of 0.992 for the fitting curve.

3.5. Specificity of the anti-PCV2-MAb immobilized Ex-TFG

In order to assess the specificity of the proposed sensor, the fully PCV2-combined Ex-TFG was treated with the above

dissociation method, and recombined with anti-PCV2 MAbs using the highly purified anti-PCV2-MAb solution (0.08 mg/mL in PBS). Then, a control experiment was carried out with the prepared PRRSV solution (5µg/mL in PBS) and PCV2 solution ($1.154×10^4$ $TCID_{50}$/mL in PBS) as the first and following binding targets, respectively.

In addition, the above experiment for evaluating the sensor specificity was repeated once more, using totally identical method and conditions. Resonance wavelength variation for the whole process is shown in Fig. 6(c), where the resonance wavelength after the first anti-PCV2 MAb dissociation from the fiber surface is set as a reference point, indicating that the anti-PCV2-MAb immobilized Ex-TFG sensor does not respond to the PRRSV target but undergoes an obvious wavelength change (~0.19 nm) in the case of PCV2.

4. Conclusions

We developed a label-free immunosensor based on SPA-modified Ex-TFG inscribed in SM28 fibers for specific, fast and stable detection of PCV2. Steady and obvious resonance wavelength shift, about 0.23 nm, could be observed as the PCV2 titer level changed from 0 to ~$1.154×10^4$ $TCID_{50}$/mL. The saturation value of the PCV2 immunosensor was ~$4.801×10^3$ $TCID_{50}$/mL (i.e. $2.08×10^3$ ng/mL), and LOD of ~9.371 $TCID_{50}$/mL (i.e. ~4.06 ng/mL) for PCV2 was obtained, which was much better than that (0.04µg/mL) of the optoelectronic SPR method (Hu et al., 2014). In addition, the proposed immunosensor showed a good repeatability and an excellent specificity for PCV2 detection. Although the LOD of the proposed PCV2 immunosensor is not as high as that (LOD of ~1$TCID_{50}$/mL) of the most recently reported PCR-based detection (Chang et al., 2014), the more convenient operation, shorter detection time, more stable results, and no expensive reagent or experimental instrument are all advantages compared with the PCR-based methods. However, the resonance wavelength only changed ~0.02 nm at its LOD titer level, actually the sensitivity of the immunosensor could be further improved. Therefore, future research will focus on improving the LOD and sensitivity of the proposed label-free immunosensor, which could be realized by using Ex-TFG inscribed in a thin-cladding optical fiber (SM1500 fiber) as a bio-sensing platform (Yan et al., 2015; Luo et al., 2015).

References

Wang, X. and Otto, S. W., 2013. Anal. Chem. 85, 487-508.

Fan, X. D., Ian, M. W., Siyka, I. S., Zhu, H., Jonathan, D. S., Sun Y., 2008. Analytica Chimica Acta 620, 8-26.

Tian, Y., Wang, W., Wu, N., Zou, X., Wang X., 2011. Sens. 11, 3780-3790.

Cao, J., Minh, H. T., Sun, T., Kenneth, T. V., 2013. Sens. and Actuators B 181, 611-619.

He, Z., Tian, F., Zhu, Y., Lavlinskaia, N., Du, H., 2011. Biosen. and Bioelectron. 26, 4774-4778.

Luo, B., Yan, Z., Sun, Z., Li, J., Zhang, L., 2014. Opt. Express 22(25), 30571-30578.

Tischer, I., Gelderblom, H., Vettermann, W., Koch, M. A., 1982. Nature 295, 64-66.

Pejsak, Z., Podgo´rska, K., Truszczyn´ski, M., Karbowiak, P., Stadejek, T., 2010. Comp. Immunol. Microbiol. Infect. Dis. 33, e1-e5.

Ge, X. N., Wang, F., Guo, X., Yang, H. C., 2012. Virus Res. 164, 100-106.

Gilpin, D. F., McCullough, K., Meehan, B. M., McNeilly, F., McNair, I., Stevenson, L. S., Foster, J. C., Ellis, J. A., Krakowka, S., Adair, B. M., Allan, G. M., 2003. Vet. Immunol. Immunopathol. 94(3-4), 149-161.

Ian, W. W., Carrie, A. K., Victoria, A., Jewhurst, I. M., Francis M., Brian, M. M., Tiffany, S. C., John, A. E., Gordon, M. A., 2000. J. Vet. Diagn. Invest. 12, 400-405.

Eva, P., Albert, R., Maria, C., Annette, M., Fernando, R., Joaquim, S., 2007. Journal of Virological Methods 146 86-95.

Caprioli, A., McNeilly, F., McNair, I., Lagan-Tregaskis, P., Ellis, J., Krakowka, S., McKillen, J., Ostanello, F., Allan, G., 2006. Res. Vet. Sci. 81, 287-292.

Kathleen, A. M., Anju, T., John, C. S., Harding, Steven, K., John, A. E., Janet E. H., 2009. Veterinary Microbiology 133, 23-33.

Chang, C.Y., Deng, M.C., Wang, F.I., Tsai, H.J., Yang, C.H., Chang, C., Huang, Y.L., 2014. J. Virol. Methods. 201, 13-19.

Park, C., Kim, B. S., Kim, Y. H., Cho, H. S., 2011. Korean J. Vet Serv. 34(1), 1-4.

Hu, J. D., Wang, T. T., Wang, S., Chen, M. W., Wang, M. P, Mu, L. Y., Chen, H. Y., Hu, X. R., Liang, H., Zhu, J. H., Jiang, M., 2014. PLOS ONE 9(10), e111292-1~e111292-6.

Sjoquist, J., Meloun, B., Hjelm, H., 1972. Eur. J. Biochem. 29(3), 572-578.

Kangwa, M., Yelemane, V., Polat, A. N., Gorrepati, K. D., Grasselli, M., Fernández-Lahore, M., 2015. AMB Express 5, 70-79.

Zhou., K., Zhang, L., Chen, X., Bennion, I., 2006. Opt. Lett. 31(9), 1193-1195.

Shu, X. W., Zhang, L., Bennion, I., 2002. J. Lightwave Technol. 20(2), 255-266.

Andreeva, AL, Andreev OA, Borejdo J., 1993. Biochemistry 32(50), 13956-13960.

Hong, J., Xu, D., Gong, P., Sun, H., Dong, L., Yao, S., 2007. J. Molecular Catalysis B: Enzymatic 45, 84-90.

Trang, H. K., Schadock-Hewitt, A. J., Jiang, L., Marcus, R. K., 2016. J. Chromatography B 1015-1016, 92-104.

Abani K. B., 2002, Biochemistry 41, 13386-13394.

König, B., Grätzel, M., 1994. Anal. Chem. 66(3), 341-344.
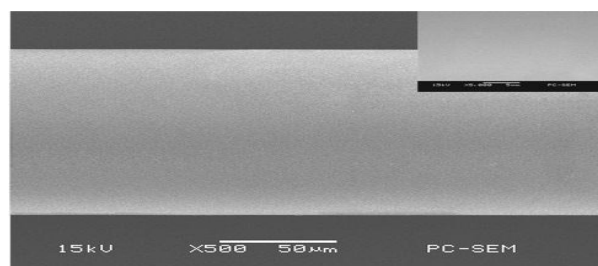
Wang, H., Liu, Y., Yang, Y., Deng, T., Shen, G., Yu, R. A., 2004. Anal. Biochem. 324(2), 219-226.

Yan, Z., Sun, Z., Zhou, K., Luo, B., Li, J., Wang, H., Wang, Y., Zhao, W., Zhang, L., 2015. J. Lightwave Technol. 33(14), 3023-3027.
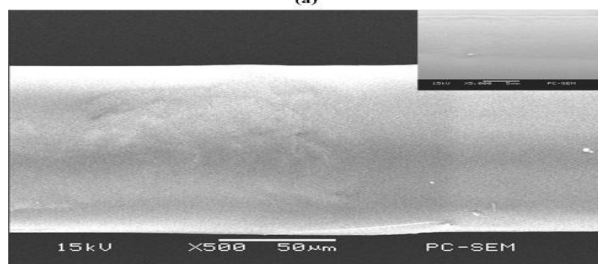
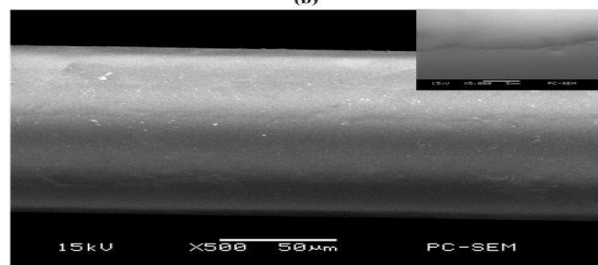Luo, B., Yan, Z., Sun, Z., Liu, Y., Zhao, M., Zhang, L., 2015. Opt. Express 23(25), 32429-32440.
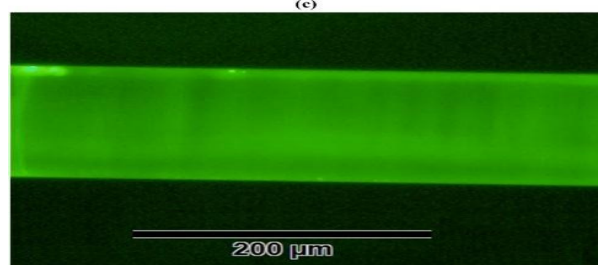
Graphical abstract

(a)

(b)

(c)

(d)